Standoff raman spectroscopy system for remote chemical detection.

E.C. Cull, M.E. Gehm, B.D. Guenther, and D.J. Brady

Duke University Fitzpatrick Center for Photonics and Communications Systems, Durham, NC 27708

ABSTRACT

We have developed a class of aperture coding schemes for Remote Raman Spectrometers (RRS) that remove the traditional trade-off between throughput and spectral resolution. As a result, the size of the remote interrogation region can be driven by operational, rather than optical considerations. In this paper we present the design of our coded-aperture standoff spectroscopy system as well as experimental data collected while making remote measurements.

Keywords: remote sensing, Raman spectroscopy, multiplex measurement, chemical detection, coded aperture

1. INTRODUCTION

Currently, security and environmental applications demand systems capable of remote chemical detection.[1] Standoff detection systems based on Remote Raman Spectroscopy (RRS) have been demonstrated and are used in numerous areas, including explosives detection, atmospheric analysis, and detection of different organic and inorganic compounds.[2,3] An RRS system has two key parts. The first is a monochromatic excitation source (a laser, or lasers) and the second is a spectrometer. The system works by projecting excitation laser light onto the target of interest, thereby generating Raman photons. A telescope then collects the scattered Raman photons and couples them into the spectrometer for analysis. A schematic of this kind of system is shown in Fig. 1. The spectrum of the Raman scattered photons contains features which can be used to uniquely identify trace chemical compounds on the target. The light becomes an "optical fingerprint" of the chemical environment at the target.

The interrogation region is the area illuminated by the excitation laser on the target of interest. This region acts as an incoherent source of Raman photons. These photons are emitted along an isotropic angular profile, and the spatial extent of this region can be defined by optics in front of the excitation laser. When working with incoherent sources like those generated by the RRS excitation laser, traditional spectrometers have an inherent trade-off between throughput and spectral

Further author information: Send correspondence to dbrady@duke.edu

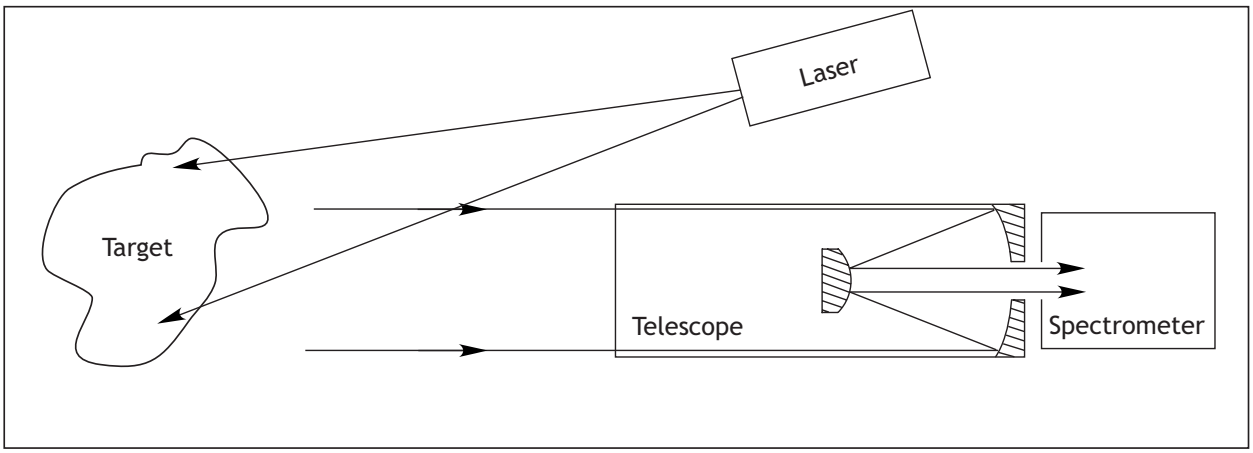

Figure 1. Typical optical system schematic for an RRS.

Chemical and Biological Sensors for Industrial and Environmental Security, edited by Arthur J. Sedlacek, Steven D. Christesen, Roger J. Combs, Tuan Vo-Dinh, Proc. of SPIE Vol. 5994, 59940H, (2005)
0277-786X/05/$15 · doi: 10.1117/12.626170

resolution caused by the spatial-filtering of the slit at the spectrometer's input aperture. In RRS, however, the light collected by the telescope is significantly spatially-filtered by the small solid angle the telescope aperture subtends as seen from the target. This makes it possible, in certain circumstances, to focus the excitation laser to a small enough interrogation region such that the telescope can focus the collected Raman photons completely into a slit based spectrometer. (This spot size is typically on the order of 1mm).[4] This, however, presents a set of problems. Focusing a laser to a small spot can create dangerously high power densities on the target. It can be difficult to focus an excitation spot to a sufficiently small area given environmental scattering effects such as the atmospheric scattering of UV light (for a UV excitation source) or simply smoke and/or dust in the target region. A small interrogation region also presents problems when using RRS in a scanning mode. It could take a significant amount of time to scan a large area for some chemical of interest with a 1 mm interrogation region. Using a larger interrogation with a traditional slit spectrometer requires a tradeoff between poor light throughput with a narrow slit and poor spectral resolution with a wide slit.

We have developed a series of aperture codes for spectrometers that break this relationship between light throughput and spectral resolution, thus allowing the system designer to optimize each independently.[5] These aperture codes implement a form of multiplex measurement, and the resulting system is a computational optical sensor—the measurement is no longer isomorphic to the input signal. Instead, algorithmic methods must be employed to extract the spectrum from the measurement. The result is an instrument that is significantly more flexible than traditional spectrometers.

In the context of remote chemical detection, this flexibility is primarily useful in allowing the size of the interrogation region to be controlled by operational requirements. For instance, we can increase the area of the target scanned for a particular measurement and / or we can control the power density of the excitation laser on the target. Consequently, instruments designed along these lines should prove significantly more useful in true operational environments.

This paper begins with a brief overview of Raman spectroscopy and its application to chemical detection. Next, we describe the basic theory of a coded aperture spectrometer, followed by the design and implementation of our RRS system. Finally, we present experimental results from remote chemical measurements made with our RRS system.

2. RAMAN SPECTROSCOPY

Light scattered from atoms or molecules can be used to extract a vast amount of information about the scattering objects. The majority of the light scatters with the same energy that it had originally (when viewed in a inertial reference frame traveling with the scatterer). This light is said to be *elastically scattered* or *Rayleigh scattered*. When the spectrum of elastically scattered light is viewed from a reference frame *not* traveling with the scatterer, the light will be seen to have shifted in frequency as a result of the motion of the scatterer. This is known as the *Doppler shift* and can be used to extract information on the center-of-mass motion of an ensemble of scatterers as well as the temperature of the ensemble.

Even more valuable information can be gleaned from the small fraction of light (order 10^{-5}–10^{-9}) that changes energy upon scattering (again viewed in a reference frame traveling with the scatterer). This light is said to be *inelastically scattered* or *Raman scattered*.[6] The change in energy comes from energy exchange with the internal electronic, vibrational, and rotational states of the atoms or molecules. At typical temperatures, scatters will predominantly be in the internal ground state. As a result, the most common outcome is that the scattered light loses energy to the scatterer and emerges at a longer wavelength. This is known as the *Stokes component*. With high temperature, or otherwise energetically excited scatters, the light can scatter with an increase of energy, and concomitant shorter wavelength. This is the *anti-Stokes component*. The change in the wavelength of the light (to either longer or shorter wavelength) is known as the *Raman shift*. A schematic of a Stokes Raman scattering event is shown in Fig. 2. The solid lines represent the rotational-vibrational levels of the target molecule. The energy difference between the incoming and outgoing photons is given by the energy difference between the two internal states. Note that the incoming photon does not excite the molecule into a true excited state, but instead the transition acts as if there has been a transition through a virtual state (dashed line).

Measurement of the spectrum of Raman scattered light will reveal a number of Raman shifts. Each shift corresponds to a particular internal state transition of the scatterer. Because the energy levels of a molecule depends crucially on the composition of the molecule, the spectrum of Raman shifts is a highly specific "fingerprint" of the internal energy level structure. As such, it can be used for extremely precise chemical detection and identification.

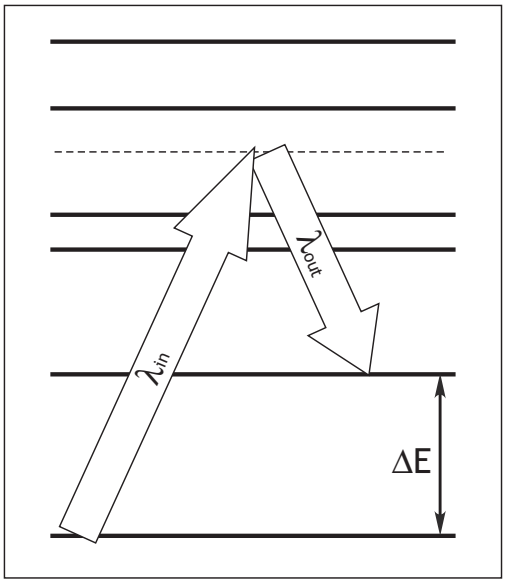

Figure 2. Schematic of a Stokes Raman transition.

3. CODED APERTURE SPECTROSCOPY

As mentioned previously, we have developed several classes of aperture-coded spectrometers that achieve high spectral resolution without sacrificing light throughput for extended sources. These spectrometers are computational optical sensors, meaning that they record some function or transformation of the spectrum instead of directly recording the spectrum. To recover spectral data from the recorded signal, the output from the detector array must first be algorithmically processed.

Our coded aperture spectrometer designs replace the input slit used in a traditional spectrometer with a two-dimensional transmission pattern known as the *aperture code* or *aperture mask*. We have developed several different sets of codes to use as our aperture codes. In this case, we chose to implement a design based on an order-n Hadamard matrix*.[7] Variations of these codes have some history in spectroscopy applications.[8] Future research will determine which type of code, Hadamard or otherwise, is optimal for RRS. A mask based on an order-24 Hadamard matrix is shown in Fig. 3.

The essential characteristic a coded aperture provides for a spectroscopic system is that the spectral resolution depends on the size of individual openings in the mask pattern, while light throughput depends on the total number of openings in the pattern. This feature decouples the tradeoff between resolution and light throughput that is present in a typical slit design where throughput varies directly with slit width and spectral resolution varies inversely with slit width.

For a traditional spectrometer, a minimum spectral resolution requires a fixed slit width, w. A system based on an order-i Hadamard-coded aperture achieves the same spectral resolution by using feature size w, but with i columns instead of the single "column" of the slit spectrometer. The Hadamard-coded mask-based approach inherently involves a 50% loss of light because half of the mask features are opaque. This means that the Hadamard-code based system achieves $i/2$ times the light throughput of the traditional system when considering a diffuse source. Further, a finer-pitched mask pattern covering the same aperture area as the original pattern maintains the same light throughput, but increases the spectral resolution of the coded aperture spectrometer. Finally, this performance is achievable at a fixed 50% throughput loss when measuring a source with large spatial extent. As a result, the choice of excitation spot size for an RRS system can be based on operational requirements rather than the optical requirements imposed by the spectrometer. A more detailed theoretical analysis of the Hadamard coded aperture versus a slit is available in Ref. 4.

*Hadamard matrices are the subset of square, unimodular, real matrices that have the maximal determinant for their size. The rows of a Hadamard matrix are mutually orthogonal, as are the columns. It can be shown mathematically that Hadamard matrices describe optimal multiplexing techniques in the presence of certain types of noise. It is conjectured that order-n Hadamard matrices exist for all n that are multiples of 4.

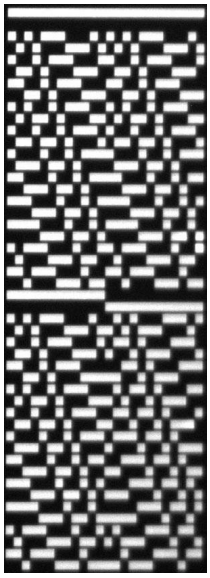

Figure 3. Microphotograph of an aperture mask (n=24).

Assuming the target spectrum is uniformly illuminating the input aperture of the spectrometer, a Hadamard-coded aperture spectrometer measures the convolution of the Hadamard matrix with the target spectrum at the detector plane. To recover the target spectrum, we take the data from the detector, subtract a dark image to reduce the pattern noise and then slightly shift each row to correct for the "smile" distortion present in grating spectrometers. The smile distortion can be easily characterized by looking at a target with distinct spectral features like a gas discharge lamp. Generally, we design our aperture mask such that a single mask element covers several pixels on the detector. The last step before inversion is to average the set of rows (along the non-dispersion axis of the spectrometer) that make up a single mask feature. The result for a mask with N rows is a set of N data vectors with length corresponding to the number of pixels along dispersion axis of the detector. A mathematical formulation of this is shown in the following equation, where $R_1 \ldots R_N$ are the data vectors from the detector, $S_1 \ldots S_N$ are spectral estimates formed for each row of input data, and **H** is the order-N Hadamard matrix.

$$\mathbf{H}_{N\times N} \begin{bmatrix} S_1 \\ \cdot \\ \cdot \\ S_N \end{bmatrix}_{N\times M} = \begin{bmatrix} R_1 \\ \cdot \\ \cdot \\ R_N \end{bmatrix}_{N\times M} . \tag{1}$$

A non-negative least squares inversion algorithm is used to calculate the spectra in $S_1 \ldots S_N$. We then average these N spectral estimates to determine the spectrum of the target.

4. CODED-APERTURE BASED REMOTE RAMAN SPECTROSCOPY SYSTEM

Our RRS system consists of an excitation laser, collection telescope, and spectrometer designed for use with both coded and slit based input apertures. The laser used with our system is a ND:YVO4 based system at 532 nm with a maximum power output of 5.5 W. The excitation laser is augmented with a narrow bandpass filter with a full width at half maximum transmission bandwidth of 2 nm. An adjustable zoom beam expander allows us to modulate the size of the excitation beam on the target. The collection telescope is a Schmidt-Cassegrain style telescope with a 254 mm aperture and f/6.3 optics.

We designed our spectrometer using the Zemax optical simulation software package. Our major design goals for the spectrometer were to target the Raman "fingerprint" region of 500 to 3000 cm^{-1} while maintaining compatibility with the optics of our collection telescope. Our spectrometer's spectral range is 546 - 645 nm, capable of measuring a Raman shift

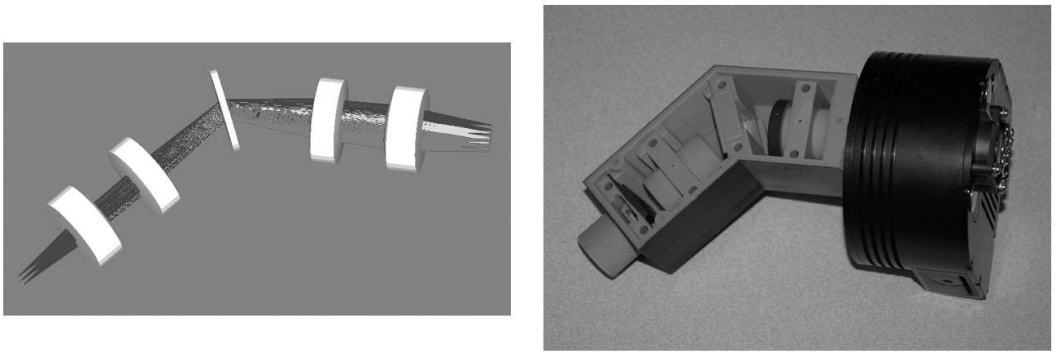

Figure 4. Diagram of the spectrometer's optics and photograph of the spectrometer.

from 480 to 3300 cm^{-1} given the 532 nm excitation laser. The device is theoretically capable of a spectral resolution of 0.13 nm / pixel, though this is practically limited by the feature size at the input aperture. The 36 μm feature size of the masks used with this device restrict our spectral resolution to approximately 0.6 nm / pixel.

The spectrometer is a fairly typical design using a transmissive holographic grating. A coded aperture mask or slit is held at the input aperture of the spectrometer, followed by a set of relay lenses which image the aperture through the holographic grating onto the CCD fixed at the output of the spectrometer. Fig. 4 shows a diagram of the optical system beside a picture of the spectrometer.

The CCD camera used with our spectrometer has a resolution of 765 x 510 and has thermoelectrically cooled focal plane. We typically operate this camera at 0^o degrees C. The mechanical structure of the spectrometer is a rigid polymer, printed by a rapid prototyping machine. It is designed to hold the optics in a light tight box which attaches to directly to the output of the telescope and the front face of the camera.

5. EXPERIMENTAL RESULTS FOR THE CODED APERTURE RRS SYSTEM

We conducted a series of tests to evaluate the performance of our coded aperture RRS system as well as to compare it to a slit based RRS system. Fig. 5 shows a picture of our RRS system. The spectrometer is mounted on the back of the 254 mm telescope and the CW excitation laser with a variable zoom beam expander is located on an optical breadboard on the floor. Our target consisted of a one gallon drum-style fish bowl with relatively flat 20 centimeter diameter sides. The target was located 30 meters downrange, measured from the input aperture of the telescope. Experiments were performed in a long hallway in the evening to minimize background lighting, but windows extending along one side of the hallway prevented the testing area from being completely dark. All experiments were performed with the laser set to 5.5 W power output with a $1/e^2$ beam size of approximately 10 centimeters on the target. This equates to a excitation laser power density on the target of 17.5 mW/cm^2, many orders of magnitude less than the power densities of $10^5 - 10^6$ W/cm^2 used in the pulsed laser experiments in Ref. 2, 3. For the tests presented in this paper, isopropanol was used as the target chemical. A typical Raman fingerprint for isopropanol is shown in Fig. 6. This spectrum was obtained with our RRS system using an order-40 Hadamard mask and a 5 second integration time.

A first set of experiments shows the spectra collected for a series of tests run with the RRS system using an order-40 Hadamard coded aperture. In these tests we varied the concentration of isopropanol at our target, diluting it with water. The integration time for the spectrometer was held constant at 60 seconds. Concentrations shown in the Fig. 7 are 100%, 50%, 25%, 12.5% and 6.25%, from top to bottom. Some features of the Raman signal are evident in the 6.25% plot, but the broad fluorescence peak noticeable above 640 nm becomes the predominant feature in the spectrum. This fluorescence is most likely caused by the glass of our sample container.

A second set of experiments run with our RRS system compare the performance of three different order coded apertures (N=12, 24 and 40) and a slit. The slit width and feature size of the masks are both 36 μm. For analysis we compare a mask to slit of equivalent height. To compare the systems, we took a spectrum with each aperture type using a 0.5 second

Figure 5. Photograph of the Remote Raman Spectroscopy System.

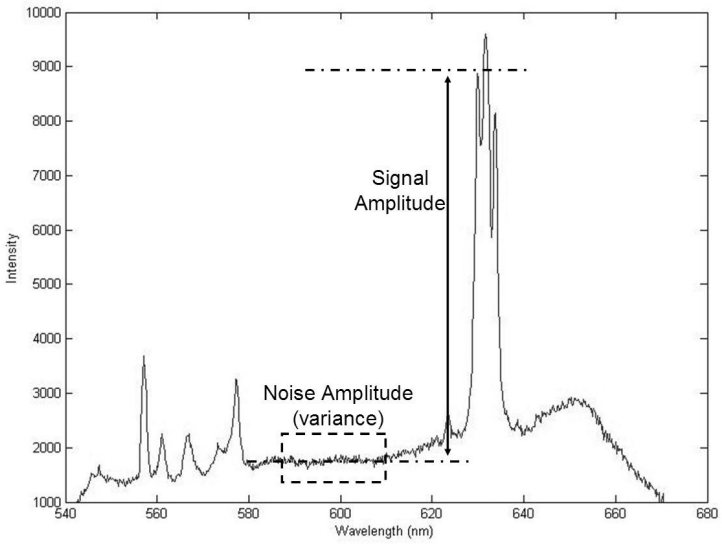

Figure 6. Raman signature of isopropanol. The plot indicates where values were taken for signal to noise calculations.

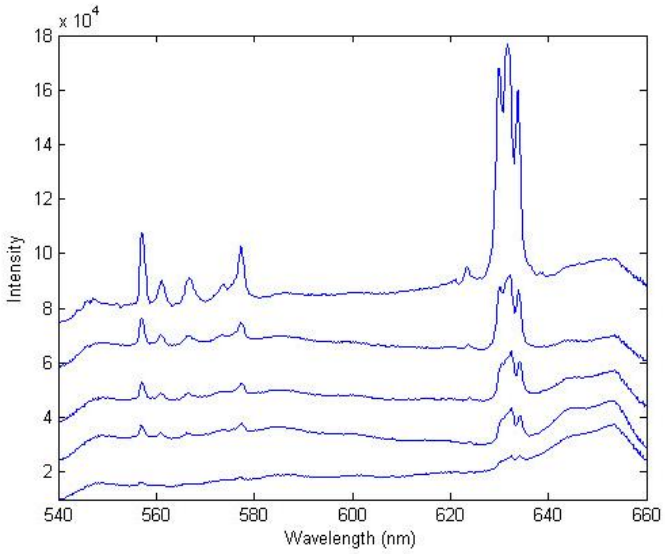

Figure 7. Raman signature of isopropanol. The plot indicates where values were taken for signal to noise calculations.

integration time. Fig. 8 shows the spectra recorded during these tests. A separate slit spectrum is plotted for each coded aperture to compare the coded aperture with a similar height slit. We used nondiluted isopropanol as the target for these experiments.

The metric used to compare the slit and three coded aperture systems is signal to noise ratio (SNR). We are not interested in the precise SNR of each spectrum, just the ratio of SNR between a coded aperture and its corresponding slit. Fig. 6 shows the definition we use for the signal amplitude and noise amplitude in the SNR calculation. Noise amplitude is taken as the variance of the spectrum over a nominally flat area (between 590 and 610 nm). The signal amplitude is taken as the height of the peak at 630 nm over the mean value of the ”flat area” between 590 and 610 nm. The ratio of the SNR of the coded aperture to that of the corresponding slit is **1.9** for the order-40 mask, **1.6** for the order-24 mask, and **1.1** for the order-12 mask.

6. SUMMARY

When performing remote chemical detection via Raman spectroscopy, the source that results is highly incoherent and several orders of magnitude less intense than the excitation light. There is also significant utility to using a large interrogation region to facilitate scanning a target area. This spatially broad and incoherent source of Raman photons forces a traditional slit spectrometer to either become light-starved or to sacrifice spectral resolution.

We have demonstrated a proof-of-concept RRS system that uses a coded aperture to simultaneously maximize light throughput to the spectrometer and maintain sufficient spectral resolution. While the system design could be further improved with the addition of a pulsed laser to increase the power intensity on the target by several orders of magnitude and a gated CCD to reject background light, it shows the advantage of a coded aperture based design versus a typical slit based spectrometer.

ACKNOWLEDGMENTS

This work was performed with the support of the Air Force Office of Scientific Research, grant number F49620-02-1-0335.

REFERENCES

1. J. P. Carrico, “Chemical-biological defense remote sensing: what’s happening,” in *Proc. SPIE Vol. 3383, Electro-Optical Technology for Remote Chemical Detection and Identification III*, pp. 45–56, Aug. 1998.

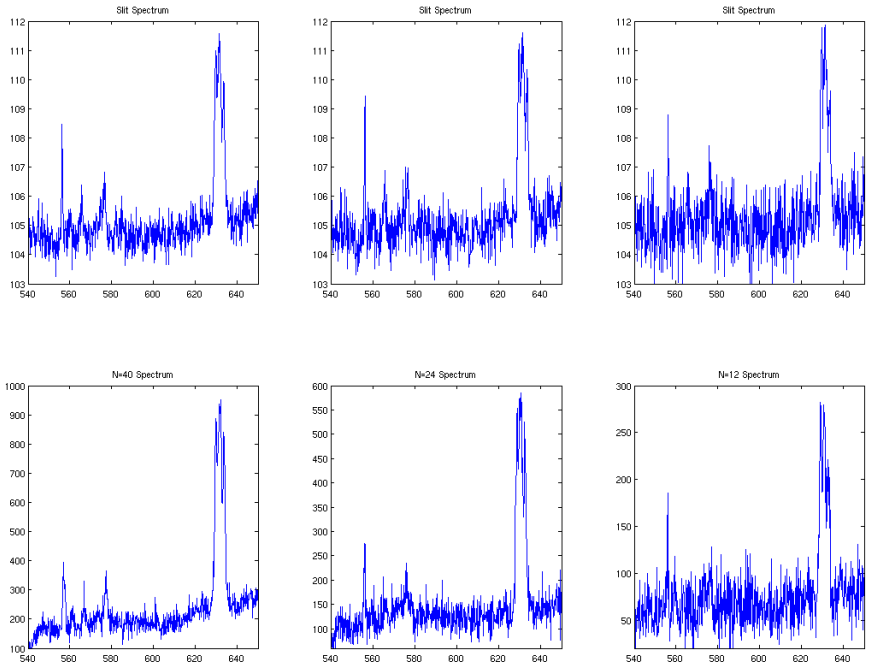

Figure 8. Raman spectra of isopropanol for 0.5 second integration, measured with a slit and Hadamard coded masks of orders 12, 24 and 40.

2. J. C. Carter, S. M. Angel, M. Lawrence-Snyder, J. Scaffidi, R. E. Whipple, and J. G. Reynolds, "Standoff detection of high explosive materials at 50 meters in ambient light conditions using a small raman instrument," *Applied Spectroscopy* **59**, pp. 769–775, 2005.
3. S. K. Sharma, P. G. Lucey, M. Ghosh, H. W. Hubble, and K. A. Horton, "Stand-off raman spectroscopic detection of minerals on planetary surfaces," *Spectrochimica Acta Part A* **59**, pp. 2391–2407, 2003.
4. E. C. Cull, M. E. Gehm, S. T. McCain, B. D. Guenther, and D. J. Brady, "Multimodal optical spectrometers for remote chemical detection," in *Proc. SPIE Vol. 5778, Sensors, and Command, Control, Communications, and Intelligence (C3I) Technologies for Homeland Security and Homeland Defense IV*, pp. 376–382, May 2005.
5. S. T. McCain, M. E. Gehm, Y. Wang., N. P. Pitsianis, and D. Brady, "Multiplex, multimodal spectrometry: Instrument design optimized for weak, diffuse sources." In progress, 2005.
6. J. R. Ferraro, K. Nakamoto, and C. W. Brown, *Introductory Raman Spectroscopy*, Academic Press, San Diego, 1994.
7. A. S. Hedayat, N. J. A. Sloane, and J. Stufken, *Orthogonal Arrays: Theory and Applications*, Springer Verlag, New York, 1999.
8. M. Harwit and N. Sloane, *Hadamard Transform Optics*, Academic Press, New York, 1979.